

In Vitro Pharmacological and Toxicological Effects of Norterpene Peroxides Isolated from the Red Sea Sponge *Diacarnus erythraeanus* on Normal and Cancer Cells

Florence Lefranc,^{†,‡} Genoveffa Nuzzo,^{‡,§} Nehal Aly Hamdy,[§] Issa Fakhri,[§] Laetitia Moreno Y Banuls,[⊥] Gwendoline Van Goietsenoven,[⊥] Guido Villani,[‡] Véronique Mathieu,[⊥] Rob van Soest,^{||} Robert Kiss,^{*,‡} and Maria Letizia Ciavatta^{*,‡}

[†]Service de Neurochirurgie, Hôpital Erasme, ULB, Route de Lennik, 1070 Brussels, Belgium

[‡]Istituto di Chimica Biomolecolare (ICB), Consiglio Nazionale delle Ricerche (CNR), Via Campi Flegrei 34, I-80078 Pozzuoli, Naples, Italy

[§]Department of Applied Organic Chemistry, National Research Center, Cairo 12613, Egypt

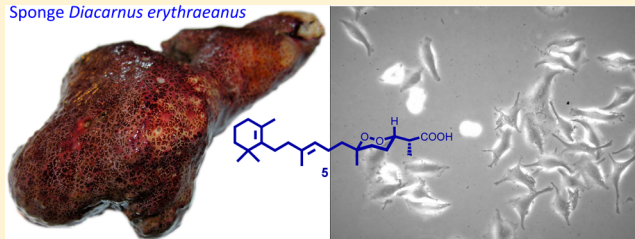
[⊥]Laboratoire de Toxicologie, Faculté de Pharmacie, Université Libre de Bruxelles, Campus de la Plaine, CP205/1, Boulevard du Triomphe, 1050 Brussels, Belgium

^{||}Department of Marine Zoology, Naturalis Biodiversity Center, P.O. Box 9517, 2300 RA Leiden, The Netherlands

S Supporting Information

ABSTRACT: Eight cyclic peroxide norterpeneoids, compounds 1–8, have been isolated and characterized from the Red Sea sponge *Diacarnus erythraeanus*, including two new norsessterterpene derivatives (3, 4). Among these metabolites, (–)-muquibilin A (5) (nine cell lines analyzed) and the new compounds 3 and 4 (seven cell lines analyzed) displayed mean IC₅₀ growth inhibitory concentrations *in vitro* of <10 μM, while the remaining compounds (1, 6–8) were inactive in these cancer cell lines. Compound 5 displayed no selectivity between normal and cancer cells in terms of *in vitro* growth inhibition. Quantitative video microscopy analysis carried out on (–)-muquibilin A-treated cells validated the data obtained by means of the MTT colorimetric assay, while flow cytometry analysis revealed ROS production but no induction of apoptosis in cancer cells.

Sponge *Diacarnus erythraeanus*



Three classes of cyclic peroxides are commonly associated with marine sponges: steroidal peroxides, norsessterterpene and norditerpene peroxides, and polyketide peroxides. Norterpene cyclic peroxides possess a 1,2-dioxane ring linked to a 2-substituted propionic acid, either free or esterified, and are characterized by an acyclic, monocyclic, or bicyclic carbon skeleton.¹ The presence of this particular class of metabolites is well documented in sponges that belong to the *Prianos*,^{2,3} *Sigmosceptrella*,^{4,5} *Mycale*,⁶ *Latrunclia*,^{7–9} *Negombata*,¹⁰ and *Diacarnus*^{11–18} genera. Among the wide array of bioactivities that have been reported for these molecules, they have been analyzed for cytotoxic effects on cancer cells^{10,11,13–18} but not on normal cells.

In this report, we present the results of the chemical investigation of the Red Sea sponge *Diacarnus erythraeanus* that led to the isolation of eight cyclic norterpene peroxides, 1–8, including six known compounds (1, 2, 5–8) and two new compounds (3, 4). The structures of the new metabolites have been elucidated by means of spectroscopic techniques, mainly NMR, mass spectrometry, and comparison with related co-occurring known norterpene. The effects on the growth of normal and cancer cells *in vitro* of these various isolated

norterpene peroxides have been evaluated by the MTT colorimetric assay. Additionally, quantitative video microscopy and flow cytometry were used to grossly decipher the mechanism of action of compound 5.

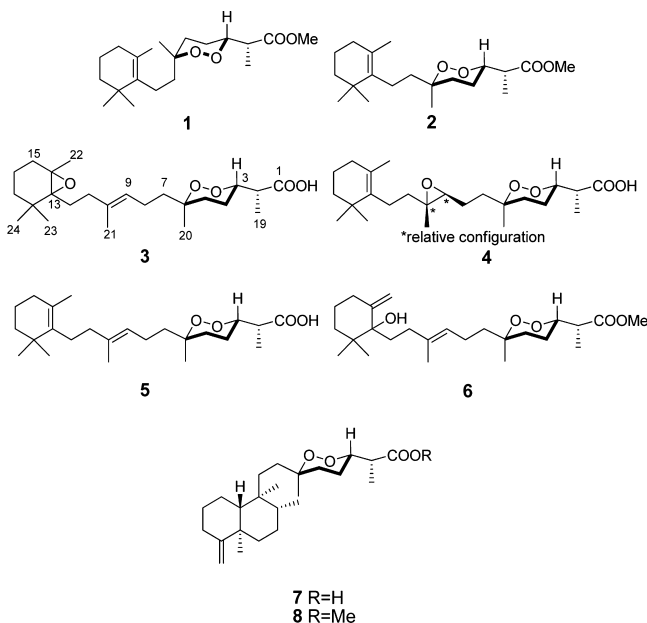
RESULTS AND DISCUSSION

The sponge *D. erythraeanus* was collected by scuba diving off Elfanadir (Hurghada Coast, Egypt) during October 2009, immediately frozen at –20 °C, and transferred to the ICB laboratory (Italy). For analysis, the frozen sponge was homogenized and extracted five times with acetone. Following concentration under reduced pressure, the aqueous residue was partitioned five times with diethyl ether and then twice with *n*-butanol. The two extracts were analyzed by TLC, which revealed a rich pattern of metabolites in the lipophilic extract. The ethereal extract (1 g) was passed through a silica gel column packed in light petroleum ether and eluted with this solvent and increasing amounts of diethyl ether to give five main fractions, A–E. Each fraction was further purified by

Received: February 4, 2013

Published: August 26, 2013

HPLC using different solvent systems as mobile phases to yield pure compounds **1** (3.0 mg), **2** (0.4 mg), **3** (1.5 mg), **4** (1.6 mg), **5** (14.4 mg), **6** (4.7 mg), **7** (33.7 mg), and **8** (4.5 mg).



A preliminary NMR analysis of the isolated compounds indicated that they all exhibited a terpenoid carbon skeleton, characterized by the presence of a cyclic peroxide. Compounds **1**, **2**, **5**, **6**, **7**, and **8** were identified as nuapapu A methyl ester (**1**),^{3,14} methyl-2-epinuapapuanate (**2**),¹⁸ (-)-muqubilin A (**5**),^{11,19} hurghaperoxide (**6**),²⁰ sigmosceptrellin B (**7**),^{4,5} and its methyl ester derivative (**8**),^{4,5} by comparing their spectroscopic data (NMR, MS, and specific rotations) with those reported in the literature. The structures of the newly identified compounds **3** and **4** were established as described below.

Compound **3** had a molecular formula of $C_{24}H_{40}O_5Na$, as deduced from the sodiated ion peak of the high-resolution mass spectrum (HRESIMS) at m/z 431.2776, indicating five degrees of unsaturation. The carbon spectrum showed 24 resonances attributable to two sp^2 olefinic carbons (one CH and one quaternary), 21 sp^3 carbons (six CH_3 , nine CH_2 , two CH, and four C), and finally a signal at δ_C 176.8 attributable to a carboxylic acid function, accounting for two of the five degrees of unsaturation as established by the molecular formula. The remaining three degrees of unsaturation indicated that compound **3** had to be tricyclic. The presence of the peroxide ring system was evident from signals at δ 4.16/81.1 (H-3/C-3) and δ_C 80.3 for C-6 common to all the known co-occurring norterpene peroxides, whereas two oxygenated carbons at δ_C 69.5 (C-13, C) and 63.6 (C-14, C) suggested the presence of a tetrasubstituted epoxide ring. The COSY spectrum of compound **3** showed similar spin systems to those found in (-)-muqubilin A (**5**). Connectivities among these systems were established through the HMBC experiment: in particular, long-range correlations of C-13 with H_3 -23, H_3 -24, H_2 -15, H_2 -12, and H_3 -22 and of C-14 with H_3 -22 and H_2 -15 allowed us to link the epoxide ring to a cyclohexane moiety and define the planar structure of **3** (Figure 1). Extensive 2D NMR experiments helped in the complete assignment of all resonances (Table 1).

The geometry of the double bond in the chain was deduced as *E*, the same as **5** and **6**, by the carbon value of the methyl linked at C-10 (δ_C 16.0, C-21). To establish the relative

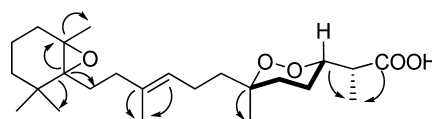


Figure 1. Selected HMBC correlations for compound **3**.

Table 1. NMR Data^a (600^b and 150^c MHz, $CDCl_3$) for Compounds **3** and **4**

position	(-)-13,14-epoxymuqubilin A (3)		(-)-9,10-epoxymuqubilin A (4)	
	δ_C , mult	δ_H (J in Hz)	δ_C , mult	δ_H (J in Hz)
1	176.8, C		177.6, C	
2	42.5, CH	2.71, dq (6.9, 6.9)	42.5, CH	2.72, m
3	81.1, CH	4.16, m ^d	80.9, CH	4.16, m ^e
4	23.3, CH_2	1.77, m	23.3, CH_2	1.81, m
5	31.9, CH_2	1.66, m	31.7, CH_2	1.68, m
6	80.3, C		79.8, C	
7	39.6, CH_2	1.54, m	39.1, CH_2	1.64, m
		1.44, m		
8	21.6, CH_2	2.12, m	22.7, CH_2	1.63, m
				1.55, m
9	123.5, CH	5.07, t (6.7)	63.2, CH	2.73, m
10	135.8, C		61.2, C	
11	36.5, CH_2	2.02, m	39.1, CH_2	1.65, m
				1.48, m
12	28.1, CH_2	1.60, m	23.9, CH_2	2.07, m
				2.02, m
13	69.5, C		136.2, C	
14	63.6, C		127.3, C	
15	30.3, CH_2	1.83, m	32.7, CH_2	1.88, m
		1.78, m		
16	17.1, CH_2	1.35, m	19.7, CH_2	1.55, m
17	36.1, CH_2	1.43, m	39.8, CH_2	1.40, m
18	34.6, C		35.0, C	
19	13.2, CH_3	1.29, d (6.9)	13.2, CH_3	1.29, d ^f
20	20.7, CH_3	1.30, s	19.5, CH_3	1.29, s
21	16.0, CH_3	1.60, br s	16.3, CH_3	1.29, s
22	22.0, CH_3	1.26, s	19.7, CH_3	1.56, br s
23	25.8, CH_3	1.04, s	28.5, CH_3	0.96, s
24	25.3, CH_3	1.01, s	28.5, CH_3	0.97, s

^aAssignments made by 1H - 1H COSY, HSQC, and HMBC. ^bFor 1H . ^cFor ^{13}C . ^d δ_H 4.52 in Pyr- d_5 , ddd, $J_{H-2-H-3} = 7.5$ Hz, $J_{H-3-H-4ax} = 8.8$ Hz, $J_{H-3-H-4eq} = 3.1$ Hz. ^e δ_H 4.50 in Pyr- d_5 , ddd, $J_{H-2-H-3} = 7.5$ Hz, $J_{H-3-H-4ax} = 8.6$ Hz, $J_{H-3-H-4eq} = 3.2$ Hz. ^fSignal partially obscured.

configuration at C-2, C-3, and C-6 of the 3-substituted 1,2-dioxane ring in our compound, Capon and Macleod's empirical rules²¹ were applied as previously adopted for this class of molecules. First, the *threo* relative configuration of carbons C-2 and C-3 carbons (2*R**, 3*S**) was suggested by the chemical shift of the methyl signal linked at C-2 resonating at δ 1.29 (H_3 -19) (a value of $\delta_H \sim 1.10$ – 1.14 was reported for a 2,3-*erythro* configuration). Second, the oxymethine H-3 proton signal appeared as an unresolved multiplet in $CDCl_3$ that was simplified to an apparent triplet ($J_{H-3/H-4ax}$ and $J_{H-3/H-4eq} \approx 6.0$ Hz) by irradiation of the vicinal H-2 proton (δ_H 2.71); this appeared different from the orientation reported in the literature for related norterpene cyclic peroxides, which mostly exhibited an axial H-3. This result prompted us to examine the stereochemical aspects of (-)-muqubilin A (**5**) and in particular the multiplicity of H-3. We thus decided to execute a decoupling experiment in different deuterated solvents:¹²

when compound **5** was dissolved in CDCl_3 , irradiation of H-2 simplified H-3 to an apparent triplet ($J_{\text{H-3}/\text{H-4ax}}$ and $J_{\text{H-3}/\text{H-4eq}} \approx 6.0$ Hz), as occurred in compound **3**; the same experiment carried out in $\text{C}_5\text{D}_5\text{N}$ simplified the proton H-3 as a double doublet ($J_{\text{H-3}/\text{H-4ax}} = 9.1$ Hz and $J_{\text{H-3}/\text{H-4eq}} = 3.2$ Hz), suggesting the axial nature of this signal; same results were obtained for compound **3** in $\text{C}_5\text{D}_5\text{N}$, suggesting an analogous orientation of H-3 (see Supporting Information). Finally, the axial orientation of the methyl at C-6 ($\delta_{\text{C}} 20.7$, H_3 -20) was deduced by its carbon resonance value (the equatorial orientation would imply a value of approximately $\delta_{\text{C}} 23$) and by the carbon value of the C-7 methylene ($\delta_{\text{C}} 39.6$ in **3** vs $\delta_{\text{C}} \sim 34$ for an equatorial orientation of the methyl at C-6). The configuration at C-13 and C-14 remained undetermined. The absolute configuration at C-2, C-3, and C-6 in **3** could be deemed to be the same as that in (–)-muqubilin A (**5**), based on biogenetic considerations. As compound **3** is an oxidized derivative of (–)-muqubilin A, the name (–)-13,14-epoxymuqubilin A is proposed.

Compound **4** presented a molecular formula of $\text{C}_{24}\text{H}_{40}\text{O}_5\text{Na}$ by HRESIMS, the same as for compound **3**. In particular, the carbon spectrum of **4** contained signals for two quaternary carbons at $\delta_{\text{C}} 136.2$ (C-13, C) and $\delta_{\text{C}} 127.3$ (C-14, C) and for two oxygenated resonances at $\delta_{\text{C}} 61.2$ (C-10, C) and $\delta_{\text{C}} 63.2$ (C-9, CH); this suggested the presence of the endocyclic double bond, as in (–)-muqubilin A (**5**), and of an epoxide group in place of the double bond in the chain. HMBC experiments helped to confirm the depicted structure of **4** (Figure 2).

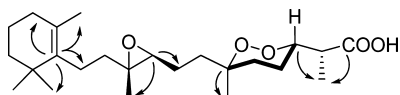


Figure 2. Selected HMBC correlations for compound **4**.

A complete assignment for this metabolite was made by careful analysis of 2D NMR experiments (COSY, HSQC, HMBC) (Table 1 and Supporting Information). The relative configurations at C-2, C-3, and C-6 of the 3-substituted-peroxide rings were deduced by the application of Capon and MacLeod's empirical rules and were assigned as $2R^*$, $3S^*$, and $6R^*$ in accordance with those of compound **3** and of (–)-muqubilin A (**5**). The relative configuration at C-9 and C-10 of the epoxide ring in the chain was suggested to be *trans* by both the carbon values of the methyl group at C-10 ($\delta_{\text{C}} 16.3$,

C-21) and the methylene at C-11 ($\delta_{\text{C}} 39.1$), compared with the same signals of *trans* and *cis* methyl-substituted epoxide models.²²

Accordingly, we propose for compound **4** the name (–)-9,10-epoxymuqubilin A.

In Vitro Growth Inhibitory Activity. Norterpene cyclic peroxides are reported to be active metabolites with varied biological activities, including antiparasitic^{12,13,16,23} and cytotoxic activity against various cancer cell lines.^{10,11,14–18} All the metabolites (with the exception of compound **2**) isolated from this sample of *Diacarnus* were analyzed for their *in vitro* growth inhibitory activity in seven cancer cell lines using the MTT colorimetric assay (Table 2). Narciclasine, podophyllotoxin, and combretastatin were used as reference compounds with respect to compound **5**, i.e., (–)-muqubilin A (Figure 3).

Of the seven compounds that were analyzed, (–)-muqubilin A (**5**) (Tables 2 and 3, and Figure 3) and the new compounds **3** and **4** (Table 2) displayed mean IC_{50} values of $<10 \mu\text{M}$, while the remaining compounds (**1**, **6–8**) were inactive ($\text{IC}_{50} > 10 \mu\text{M}$) in the seven cancer cell lines analyzed (Table 2). This observation suggests that the presence of the free acid form of these metabolites may be critical for their growth inhibitory activity in various cancer cell lines *in vitro*. However, sigmosceptrellin B (**7**), which also possesses a free carboxylic acid function, did not display the same level of growth inhibition in cancer cells as the muqubilin series of compounds (Table 2). In contrast, all the metabolites with an esterified carboxylic group displayed IC_{50} values of $>40 \mu\text{M}$ (Table 2). Although compounds **3**, **4**, and **5** [(–)-muqubilin A] displayed similar growth inhibitory activity in various cancer cell lines (Table 2), we continued our investigations with **5** because we had sufficient amounts of this compound, but not of the others, to perform additional analysis to those detailed in Table 2. Of the seven cancer cell lines for which the (–)-muqubilin A-related IC_{50} values were determined (Table 2), the Hs683 oligodendroglioma,²⁴ MCF-7 breast,²⁵ and PC-3 prostate²⁵ carcinoma cell lines displayed sensitivity to pro-apoptotic stimuli. In contrast, the U373 (Figure 3) and U251²⁶ glioblastoma, SKMEL-28 melanoma,²⁷ and A549 non-small-cell-lung cancer (NSCLC)²⁸ cell lines displayed various levels of resistance to pro-apoptotic stimuli. The data in Table 2 show that (–)-muqubilin A (**5**) displayed similar growth inhibitory activity against those cancer cell lines that are sensitive to pro-apoptotic stimuli and those cell lines that are relatively resistant to pro-apoptotic stimuli. It is therefore unlikely that (–)-muqubilin A inhibits growth by activating pro-apoptotic

Table 2. Determination of the Concentration That Causes a 50% Reduction in the Growth of a Given Cell Population Cultured *In Vitro*, Following a 72 h Incubation with the Compound of Interest (IC_{50} index in μM)^a

compound ^b	human cancer cell lines (IC_{50} in μM)							mean \pm SEM
	glioma			melanoma		carcinoma		
	Hs683	U373	U251	SKMEL28	A549	MCF-7	PC-3	
1	38	99	91	80	25	51	80	59 \pm 11
3	3	7	– ^c	22	3	6	2	7 \pm 3
4	3	4	–	15	3	4	1	5 \pm 2
5	4	7	8	8	3	7	8	6 \pm 1
6	37	83	87	73	31	45	73	56 \pm 9
7	>100	>100	>100	>100	>100	>100	>100	>100
8	35	53	54	44	24	36	44	40 \pm 4

^aThe origin and histological type of each cell line are detailed at the bottom of Table 3. ^bCompound **2** was not tested because it was not physicochemically stable. ^c“–” means not tested because too little of the compound was available.

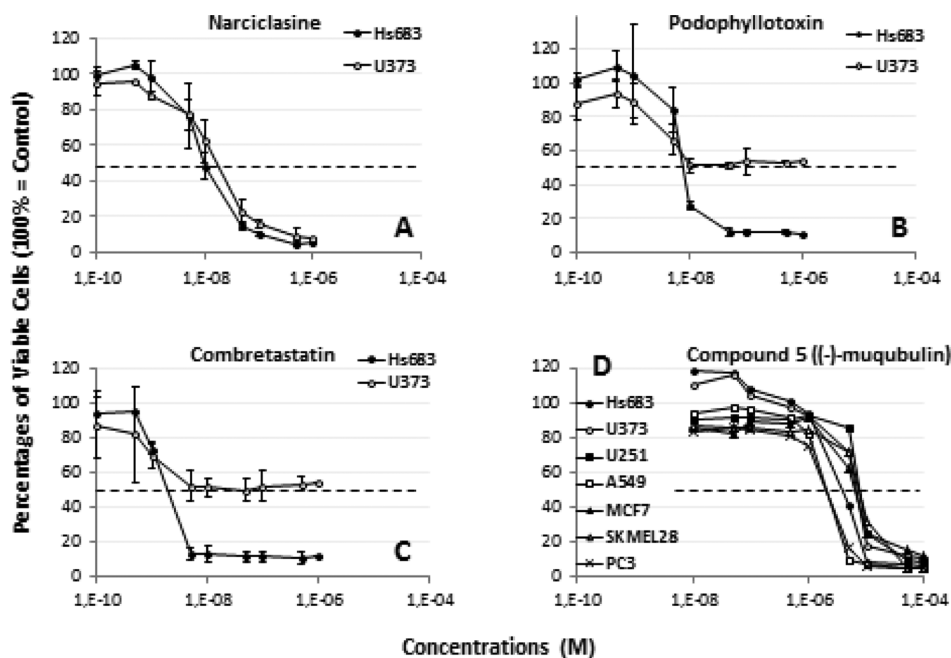


Figure 3. Characterization of the *in vitro* growth inhibitory effects (determined by means of the MTT colorimetric assay) of three reference compounds, i.e., narciclasine (A), podophyllotoxin (B), and combretastatin (C) in the human Hs683 oligodendroglioma (black dots) and U373 glioblastoma (open dots) cell lines. The data are presented as the mean \pm SEM values calculated from three independent experiments, with each experiment having been performed in six replicates. The horizontal dashed line represents 50% growth inhibition. (D) Growth inhibitory effects induced by (–)-muquubilin A in seven human cancer cell lines, namely, Hs683 oligodendroglioma, U373 and U251 glioblastoma, A549 NSCLC, MCF-7 breast and PC-3 prostate carcinoma, and SKMEL-28 melanoma cell lines. The experiment was performed once in six replicates (Table 2A), and the data are presented as mean values.

Table 3. Determination of the Concentration of (–)-Muquubilin A (5) That Causes a 50% Reduction in the Growth of a Given Cell Population Cultured *in Vitro*, Following a 72 h Incubation with the Compound of Interest (IC_{50} index in μM)^a

cancer cell lines (IC_{50} values in μM)							human normal cell lines (IC_{50} values in μM)					
human			murine				epith.			kerat.	fib.	mean \pm SEM
glioma		carcinoma			melanoma		HBL100		HaCat	NHDF	mean \pm SEM	
Hs683	U373	A549	MCF-7	PC-3	LoVo	B16F10						
7	7	6	21	15	6	3	9 \pm 2		3	23	26	17 \pm 7

^aThe origin and histological type of each cell line analyzed are as follows. Human glioma model lines included the Hs683 oligodendroglioma (ATCC code HTB-138) and the U373 (ECACC code 08061901) and U251 (ECACC code 09063001) glioblastoma cell lines. Melanoma models included the human SKMEL-28 (ATCC code HTB-72) and the mouse B16F10 (ATCC code CRL-6475) cell lines. Human carcinoma models included the A549 NSCLC (DSMZ code ACC107), the MCF-7 breast (DSMZ code ACC115), the PC-3 prostate (DSMZ code ACC465), and the LoVo colon (DSMZ code ACC350) cancer cell lines. Human normal cell lines included HBL100 epithelial (Cell Line Services code 300178), HaCat keratinocyte (Cell Line Services code 330493), and NHDF dermal fibroblasts (PromoCell code c-12300).

processes. Flow cytometry analysis confirmed these features as detailed below.

To confirm the data reported in Table 2 and to ascertain whether 5 displays selectivity between normal and cancer cells in terms of growth inhibition, we performed a second set of MTT colorimetric assay experiments as detailed in Table 3. Five of the seven cancer cell lines analyzed in this second experiment (Table 3) were the same as those analyzed during the first experiment (Table 2), but two additional cancer cell lines were analyzed, i.e., the human LoVo colon carcinoma and the mouse B16F10 melanoma cell lines. The data were very similar in these two experiments, with mean IC_{50} values ranging between 6 (Table 2) and 9 (Table 3) μM for 5. In addition, the data in Table 3 reveal that normal cells and cancer cells display similar levels of sensitivity to the growth inhibitory effects of (–)-muquubilin A (5), which leads us to conclude that (–)-muquubilin A is not selective between normal and cancer

cells. It must nevertheless be noted that the most significant differences in IC_{50} values for 5 appear to be between normal epithelial cells and keratinocytes and fibroblasts (8-fold). The HBL100 epithelial cells are transformed ones, while NHDF fibroblasts are not. HaCat keratinocytes are spontaneously immortalized cells.

Partial Deciphering of the Mechanism of Action of (–)-Muquubilin A (5). The quantitative video microscopy results, detailed in Figure 4, confirmed the data obtained from the MTT colorimetric assays (Tables 2 and 3). Specifically, 10 μM 5 decreased the growth of the three cancer cell lines analyzed, with marked effects observed as early as 24 h in U373 glioblastoma cells and in A549 NSCLC cells. As shown in Figure 4, quantitative video microscopy proved more effective in highlighting the inhibitory effects of (–)-muquubilin A than the MTT colorimetric assay (Table 2) in these two cancer cell lines. This could be because the two cancer cell lines grew faster

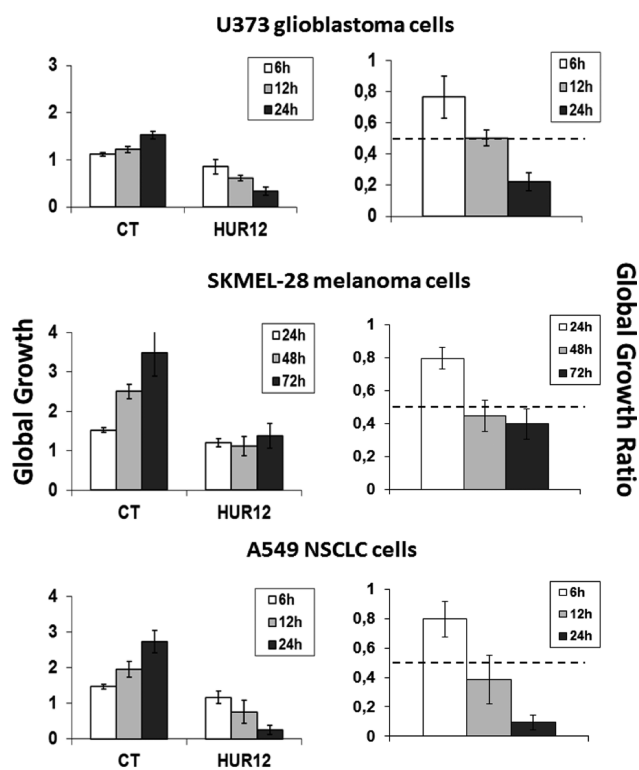


Figure 4. For each cancer cell line analyzed, a global growth ratio (the GGR index) was calculated, resulting in a value that can be directly compared to the IC_{50} value obtained from the MTT assay (the dashed horizontal line in each panel on the right). First, the global growth (GG) is calculated for each control and for each treated condition at 6, 12, and 24 h (U373 and A549) or 24, 48, and 72 h (SKMEL-28) by dividing the number of cells on the last image (at 6, 12, 24 or 24, 48, 72 h) by the number of cells on the first image. The GGR index is obtained for each cancer cell line by dividing the GG values calculated for cancer cells treated with (–)-muquibilin A by the GG values calculated for the control (untreated cells). The data are presented as the mean \pm SEM values. Each experiment was performed in triplicate.

in the T25 cm^2 flasks (a final volume of 7 mL) used for the quantitative video microscopy analysis than in the 96-well plates (a final volume of 100 μ L) used for the MTT colorimetric assay. On the other hand, quantitative video microscopy (Figure 4) and the MTT colorimetric assay (Table 2) showed similar results in the human SKMEL-28 cell line.

The results from the quantitative video microscopy analysis carried out with 10 μ M **5** in three human cancer cell lines, namely, U373²⁶ glioblastoma cells, SKMEL-28 melanoma cells,²⁷ and A549 NSCLC²⁸ cells (Figure 4), associated with various levels of resistance to pro-apoptotic stimuli, were similar in the three cancer cell lines.

Antitumor natural peroxide products are known to induce cytotoxicity in cancer cells through the generation of particular reactive oxygen species (ROS).¹⁶ Figure 5A shows that **5** also induced ROS production in Hs683 and U373 glioma cells. While both cell lines responded similarly to H_2O_2 (positive control, Figure 5A), cellular ROS content of Hs683 increased later than in U373. After 72 h of exposure, about 30% of the cells displayed increased ROS levels in both cell lines (Figure 5). However, **5**, while inducing ROS production in these two glioma cell lines, did not provoke apoptosis in these cells (Figure 5B) in comparison to narciclasine, which induced more than 85% apoptosis in PC3 prostate cancer cells after 72 h at 1

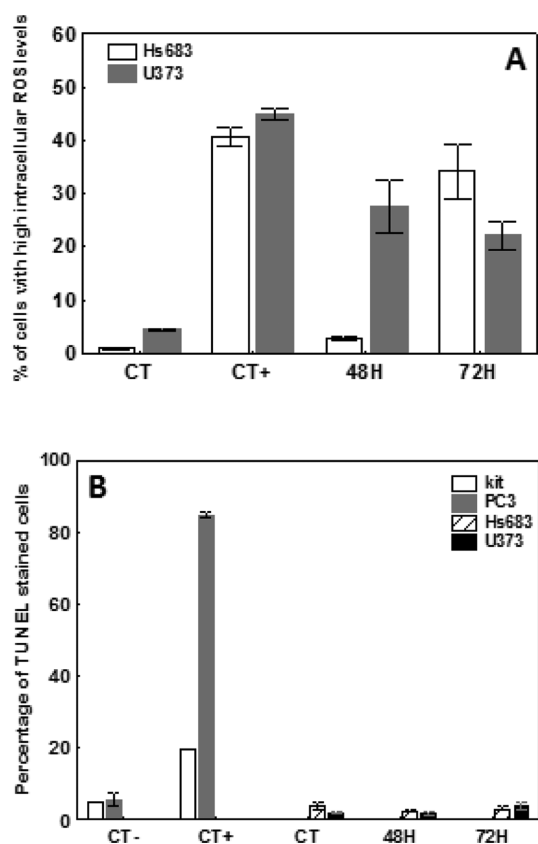


Figure 5. (A) ROS production measurements. CT refers to untreated cells, while CT+ represents cells treated for 1 h with 4 mM H_2O_2 . Results are presented as mean \pm SEM of the four replicates per experimental condition. (B) Apoptosis evaluation by TUNEL staining. White columns refer to positive and negative controls of human lymphoma cells provided with the staining kit (one replicate); gray columns refer to PC3 prostate cancer cells left untreated (CT–) or treated with 1 μ M narciclasine for 72 h (CT+; four replicates). Both Hs683 (hatched columns) and U373 (black columns) were exposed to 10 μ M (–)-muquibilin A (**5**) for 48 and 72 h before the fixation and staining procedure. Results are presented as mean \pm SEM of the four replicates per experimental condition and must be compared to their own controls, i.e., untreated cells.

μ M.²⁵ It is thus unlikely that the cytotoxic effects associated with (–)-muquibilin A (**5**) occur through induction of apoptosis. In particular, the increase in ROS production does not seem to induce apoptosis when considering U373 cells, which displayed a marked increase in ROS levels after 48 h of exposure to 10 μ M (–)-muquibilin A (**5**), while no apoptosis could be detected even after 72 h of treatment. Later time point analysis could be required to detect apoptosis in Hs683, which displayed increased ROS levels only after 72 h. These results indicate that cytotoxic (–)-muquibilin A (**5**)-mediated effects do not relate to primary apoptosis induction.

Conclusion. The current report describes the identification of eight norterpene cyclic peroxides (**1–8**), including two new compounds (**3**, **4**), from the Red Sea sponge *D. erythraeanus*. Sufficient amounts of compound **5** [(–)-muquibilin A] were available to perform toxicological and pharmacological analysis *in vitro*. Our results indicate that (–)-muquibilin A (**5**) is a cytotoxic compound without selectivity between normal and cancer cells. It induces ROS production in cancer cells, while no apoptosis was observed in the same cancer cells treated by this compound.

EXPERIMENTAL SECTION

General Experimental Procedures. Optical rotations were measured using a Jasco DIP 370 digital spectropolarimeter. IR spectra were measured on a Biorad FTS 155 FTIR spectrophotometer. 1D and 2D NMR spectra were recorded on a Bruker Avance-400 (400.13 MHz) and on a Bruker DRX-600 equipped with a TXI CryoProbe in CDCl₃ and C₆D₆ (δ values are reported and referred to CHCl₃ at 7.26 ppm and to C₆D₆ at 7.15 ppm), and ¹³C NMR spectra were recorded on Bruker DPX-300 (75 MHz) and Bruker DRX-600 (150 MHz) spectrometers (δ values are referred to CDCl₃ at 77.0 ppm and to C₆D₆ at 128.0 ppm). HRESIMS measurements were carried out on a Micromass Q-TOF micro. An HPLC Waters 501 pump with a refractometer detector was used, equipped with a normal-phase silica gel column (Ascentis Si, 5 μ m, 250 \times 4.60 mm, Supelco) and a reversed-phase column (Ascentis C-18, 5 μ m, 250 \times 4.60 mm, Supelco). TLC plates (KieselGel 60 F254) and silica gel powder (Kieselgel 60 0.063–0.200 mm) were from Merck. Solvents for chromatography were HPLC grade and were used without further purification. Human and murine normal and cancer cell lines were obtained from the American Type Culture Collection (ATCC, Manassas, VA, USA), the European Collection of Cell Culture (ECACC, Salisbury, UK), the Deutsche Sammlung von Mikroorganismen und Zellkulturen (DSMZ, Braunschweig, Germany), Cell Line Services (Eppelheim, Germany), Lonza (Vervier, Belgium), and PromoCell GmbH (Heidelberg, Germany). The code number and histological type of each of the cell lines used in the current study are detailed in Table 3.

Collection of the Animal Material. The sponge *Diacarnus erythraeanus* was collected by G.V. using scuba at a depth of 10 m off Elfanadir, Hurghada Coast, Red Sea (Egypt), in October 2009. A voucher specimen of *D. erythraeanus* was identified by R.v.S.²⁹ and is deposited in the Naturalis Biodiversity Center of Leiden (The Netherlands) with the code RMNH Por. 6200.

The sponge is repent and has a conulose surface. The skeleton consists of thick spicule bundles in the choanosomal region that subdivide into discrete thinner bundles of approximately 150–300 μ m diameter, and these in turn divide into finer tracts of approximately 15–20 μ m diameter near the surface. There are also loose spicules scattered everywhere in low proportions. The spicules are thin strongyles and subtylostongyles, approximately 235–275 by 2.5–3 μ m in size, and very rare spinorhabds of 25 by 3 μ m. This combination of properties conforms closely to the description of the holotype of *D. erythraeanus*.

Extraction of the Sponge *D. erythraeanus* and Isolation of Norterpene Peroxides (1–8). The frozen sample of *D. erythraeanus* (16 g, dry weight) was extracted with acetone (5 \times 500 mL). The acetone extracts were concentrated *in vacuo*, and the aqueous residue was first fractionated between H₂O and Et₂O (5 \times 250 mL), then with *n*-BuOH (2 \times 200 mL). Following evaporation under reduced pressure, we obtained 1 g of ethereal extract and 0.5 g of butanol extract. The sponge ethereal extract was then subjected to silica gel chromatography, eluting with light petroleum and increasing amounts of diethyl ether. The resulting fractions were combined on the basis of their chromatographic homogeneity to afford five main fractions, A to E, which were further subjected to HPLC. Fraction A (eluted from the silica gel column with light petroleum/diethyl ether, 8:2), after purification on NP-HPLC (*n*-hexane/EtOAc, 99:1, flow 1.3 mL/min), yielded the norditerpene nuapapuina methyl ester (1, formerly known as methyl nuapapuanoate) and methyl-2-epinuapapuanoate (2). This fraction also contained the norsesiterpene 8, recognized as sigmosceptrellin B methyl ester. Fractions B–E were further purified on a RP-18 HPLC column using MeOH/H₂O (9:1) as mobile phase. In particular, hurghaperoxide (6) was isolated from both fractions B and C (eluted with petroleum ether/diethyl ether, 7:3 and 1:1, respectively). The new compounds 3, 4, (–)-muqubilin A (5), and sigmosceptrellin B acid (7) were purified from both fractions D and E (eluted with petroleum ether/diethyl ether, 4:6, and diethyl ether, respectively).

(–)-13,14-Epoxy muqubilin A (3): colorless oil; [α]_D²⁵ –47.8 (c 0.10, CHCl₃); IR (liquid film) ν_{\max} 3400, 1700, 1495, 1380 cm^{–1}; ¹H

NMR and ¹³C NMR in CDCl₃, see Table 1; HRESIMS *m/z* 431.2776 [M+ Na]⁺ (calcd for C₂₄H₄₀O₅Na, 431.2773).

(–)-9,10-Epoxy muqubilin A (4): colorless oil; [α]_D²⁵ –26.2 (c 0.20, CHCl₃); IR (liquid film) ν_{\max} 3400, 1700, 1495, 1380 cm^{–1}; ¹H NMR and ¹³C NMR in CDCl₃, see Table 1; HRESIMS *m/z* 431.2770 [M+ Na]⁺ (calcd for C₂₄H₄₀O₅Na, 431.2773).

(–)-Muqubilin A (5): colorless oil; [α]_D²⁵ –32.7 (c 0.34, CHCl₃); lit.¹¹ [α]_D –31.6 (c 0.18, CHCl₃); ¹H and ¹³C NMR spectra, see the SI.

Reference Compounds. Narciclasine was a generous gift from Prof. Antonio Evidente (University Federico II, Naples, Italy), while combretastatin and podophyllotoxin were generous gifts of Prof. Alexander Kornienko (Department of Chemistry and Biochemistry, Texas State University, San Marco, TX, USA).

Cell Line Cultures. The U373, U251, Hs683, SKMEL-28, B16F10, A549, PC-3, LoVo, HBL100, and HaCat cell lines were cultured in RPMI culture medium (Lonza; code 12-115F) supplemented with 10% heat-inactivated fetal bovine serum (Lonza, FBS South America code DE14-801F). Cell culture media were supplemented with 4 mM glutamine (Lonza code BE17-605E), 100 μ g/mL gentamicin (Lonza code 17-5182), and penicillin–streptomycin (200 units/mL and 200 μ g/mL) (Lonza code 17-602E). The NHDF fibroblasts were cultured in Lonza medium (CC3132 KT FGM-2 BulletKit).

Determination of the IC₅₀ Growth Inhibitory Concentrations *in Vitro*. The MTT colorimetric assay was used as detailed previously.^{25,27} Briefly, this test measures the number of metabolically active cells that are able to transform the yellow substrate 3-(4,5-dimethylthazol-2-yl)-2,5-diphenyltetrazolium bromide (MTT) into the blue formazan dye via a mitochondrial reduction involving succinate dehydrogenase. The amount of formazan obtained at the end of the experiment (measured by spectrophotometry) is directly proportional to the number of living cells. The determination of the optical density in the control compared to the treated cells helps measure the effects of compounds on the growth of normal as well as cancer cells *in vitro*. Each experimental condition was assessed in six replicates.

Computer-Assisted Phase-Contrast Microscopy (Quantitative Video Microscopy) Analysis. The direct visualization of anticancer effects induced by compound 5 [(–)-muqubilin A] in human U373 glioblastoma, SKMEL-28 melanoma, and A549 NSCLC cells was performed as detailed elsewhere.²⁷

Flow Cytometry Analysis for ROS Measurements. ROS intracellular content was evaluated through their reaction with the reduced and deacetylated form of 2',7'-dichlorodihydrofluorescein diacetate (DCFH-DA, Sigma-Aldrich) once inside the cell. The emitted fluorescence is measured by flow cytometry with a Cell Lab Quanta apparatus (Beckman Coulter). Briefly, after the exposure of Hs683 and U373 glioma cells to 10 μ M (–)-muqubilin A (5) for 48 and 72 h or to 4 mM H₂O₂ for 1 h as positive control, cells were incubated with 20 μ M DCFH-DA in RPMI without phenol red medium for 1 h at 37 °C. Living cells were then washed twice and detached for further fluorescence analysis. The experiment was conducted once in quadruplicate.

Flow Cytometry Analysis for Apoptosis Measurements. Apoptosis induction was evaluated by TUNEL staining using the APO-Direct BD Pharmingen kit following the manufacturer's instructions. Apart from the negative and positive controls provided with the kit, we made use of PC3 human prostate cancer cells left untreated or treated with 1 μ M narciclasine as negative and positive controls, respectively.²⁵ The experiment was conducted once in quadruplicate with U373 and Hs683 cells.

ASSOCIATED CONTENT

Supporting Information

¹H and ¹³C NMR, ¹H–¹H COSY, HSQC, HMBC, and NOESY spectra of compounds 3 and 4 and ¹H and ¹³C NMR spectra of compound 5 are available free of charge via the Internet at <http://pubs.acs.org>.

AUTHOR INFORMATION

Corresponding Authors

*Chemistry: E-mail: lciavatta@icb.cnr.it. Tel: +39 081 8675243.

*Pharmacology and toxicology: E-mail: rkiss@ulb.ac.be. Tel: +32 477 622 083.

Author Contributions

#The first two authors equally contributed to this work.

Notes

The authors declare no competing financial interest.

ACKNOWLEDGMENTS

The authors sincerely acknowledge Mrs. D. Melck and Mr. V. Mirra of the ICB-NMR staff service, Mr. C. Iodice for spectrophotometric measurements, and Mrs. R. Arciprete and Mr. F. Castelluccio for the technical work. This work was supported by a bilateral cooperation program between CNR (Italy) and ASRT (Egypt). The Fonds National de la Recherche Scientifique (FNRS, Belgium) supported R.K. as a director of research and L.M.B. (Aspirante FNRS) and G.V.G. (Grant Télévie) as Ph.D. students. We thank H. Leclercqz for her help with respect to some of the MTT test-related experiments. This work was partially supported by PRIN-MIUR 2009 Project "Natural products and bioinspired molecules interfering with biological targets involved in control of tumor growth" and by the Belgian Brain Tumour Support (BBTS, Belgium).

REFERENCES

- (1) Casteel, D. A. *Nat. Prod. Rep.* **1992**, *60*, 289–312.
- (2) Kashman, Y.; Rotem, M. *Tetrahedron Lett.* **1979**, *19*, 1707–1708.
- (3) Manes, L. V.; Bakus, G. J.; Crews, P. *Tetrahedron Lett.* **1984**, *25*, 931–934.
- (4) Albericci, M.; Collart-Lempereur, M.; Braekman, J. C.; Daloz, D.; Tursch, B.; Declercq, J. P.; Germain, G.; Van Meerse, M. *Tetrahedron Lett.* **1979**, *19*, 2687–2690.
- (5) Albericci, M.; Braekman, J. C.; Daloz, D.; Tursch, B. *Tetrahedron* **1982**, *38*, 1881–1890.
- (6) Capon, R. J.; Rochfort, S. J.; Ovenden, S. P. B. *J. Nat. Prod.* **1997**, *60*, 1261–1264.
- (7) Capon, R. J.; MacLeod, J. K.; Willis, A. C. *J. Org. Chem.* **1987**, *52*, 339–342.
- (8) He, H. J.; Faulkner, D. J.; Lu, H. S. M.; Clardy, J. *J. Org. Chem.* **1991**, *56*, 2112–2115.
- (9) Ovenden, S. P. B.; Capon, R. J. *Aust. J. Chem.* **1998**, *51*, 573–579.
- (10) Chao, C. H.; Chou, K. J.; Wang, G. H.; Wu, Y. C.; Wang, L. H.; Chen, J. P.; Sheu, J. H.; Sung, P. J. *J. Nat. Prod.* **2010**, *73*, 1538–1543.
- (11) Sperry, S.; Valeriote, F. A.; Corbett, T. H.; Crews, P. *J. Nat. Prod.* **1998**, *61*, 241–247.
- (12) D'Ambrosio, M.; Guerriero, A.; Denaro, E.; Debitus, C.; Munoz, V.; Pietra, F. *Helv. Chim. Acta* **1998**, *81*, 1285–1292.
- (13) El Sayed, K. A.; Hamann, M. T.; Hashish, N. E.; Shier, W. T.; Kelly, M.; Khan, A. A. *J. Nat. Prod.* **2001**, *64*, 522–524.
- (14) Youssef, D. T. A.; Yoshida, W. Y.; Kelly, M.; Scheuer, P. J. *J. Nat. Prod.* **2001**, *64*, 1332–1335.
- (15) Youssef, D. T. A. *J. Nat. Prod.* **2004**, *67*, 112–114.
- (16) Dai, J.; Liu, Y.; Zhou, Y. D.; Nagle, D. G. *J. Nat. Prod.* **2007**, *70*, 130–133.
- (17) Ibrahim, S. R. M.; Ebel, R.; Wray, V.; Müller, W. E. G.; Edrada-Ebel, R.; Proksch, P. *J. Nat. Prod.* **2008**, *71*, 1358–1364.
- (18) D'Ambrosio, M.; Guerriero, A.; Debitus, C.; Waikiedre, J.; Pietra, F. *Tetrahedron Lett.* **1997**, *38*, 6285.
- (19) In accord with ref 11 we named compound **5** as (–)-muqubilin A (i.e., *ent*-muqubilin).
- (20) Guo, Y. W.; Gavagnin, M.; Mollo, E.; Cimino, G.; Hamdy, N. A.; Fakhri, I.; Pansini, M. *Nat. Prod. Lett.* **1996**, *9*, 105–112.
- (21) Capon, R. J.; MacLeod, J. K. *Tetrahedron* **1985**, *41*, 3391–3404.
- (22) Searle, P. A.; Molinski, T. F. *Tetrahedron* **1994**, *50*, 9893–9908.
- (23) Rubio, B. K.; Tenney, K.; Ang, K. H.; Abdulla, M.; Arkin, M.; McKerrow, J. H.; Crews, P. *J. Nat. Prod.* **2009**, *72*, 218–222.
- (24) Branle, F.; Lefranc, F.; Camby, I.; Jeuken, J.; Geurts-Moespot, A.; Sprenger, S.; Sweep, F.; Kiss, R.; Salmon, I. *Cancer* **2002**, *95*, 641–655.
- (25) Dumont, P.; Ingrassia, L.; Rouzeau, S.; Ribaucour, F.; Thomas, S.; Roland, I.; Darro, F.; Lefranc, F.; Kiss, R. *Neoplasia* **2007**, *9*, 766–776.
- (26) Li, J.; Hu, W.; Lan, Q. *J. Neurooncol.* **2012**, *110*, 187–194.
- (27) Debeir, O.; Van Ham, Ph.; Kiss, R.; Decaestecker, C. *IEEE Trans. Med. Imaging* **2005**, *24*, 697–711.
- (28) Mathieu, A.; Rummelink, M.; D'Haene, N.; Penant, S.; Gaussin, J. F.; Van Ginckel, R.; Darro, F.; Kiss, R.; Salmon, I. *Cancer* **2004**, *101*, 1908–1918.
- (29) van Soest, R. *Diacarnus erythraeanus*. In World Porifera database, 2012. Van Soest, R. W. M., Boury-Esnault, N., Hooper, J. N. A., Rützler, K., de Voogd, N. J., Alvarez de Glasby, B., Hajdu, E., Pisera, A. B., Manconi, R., Schoenberg, C., Janussen, D., Tabachnick, K. R., Klautau, M., Picton, B., Kelly, M., Vacelet, J., Dohrmann, M., Eds.; Accessed through World Register of Marine Species at <http://www.marinespecies.org/aphia.php?p=taxdetails&id=168712>.